Asserting the Precise Position of 3D and Multispectral Acquisition Systems for Multisensor Registration Applied to Cultural Heritage Analysis

Camille Chane Simon, Rainer Schütze, Frank Boochs, Franck S. Marzani

Asserting the Precise Position of 3D and Multispectral Acquisition Systems for Multisensor Registration Applied to Cultural Heritage Analysis

Camille Simon[1,2], Rainer Schütze[2], Frank Boochs[2], and Franck S. Marzani[1]

[1] le2i, Université de Bourgogne, Dijon, France
camille.simon,franck.marzani@u-bourgogne.fr
[2] i3mainz, Mainz University of Applied Sciences, Mainz, Germany
camille.simon,rainer.schuetze,boochs@geoinform.fh-mainz.de

Abstract. We present a novel method to register multispectral acquisitions on a 3D model. The method is based on the external tracking of the acquisition systems using close-range photogrammetric techniques: multiple calibrated cameras simultaneously observe the successive acquisition systems in use. The views from these cameras are used to precisely determine the position of each acquisition system. All datasets can then be projected in the same coordinate system. The registration is thus independent from the quality and content of the data. This method is well suited to the study of cultural heritage or any other application where we do not wish to place targets on the object. We describe the method and the simulation pipeline used to find an adequate setup for two case studies.

Keywords: 2D-3D registration, close range photogrammetry, optical calibration, 3D digitization, multispectral acquisitions, cultural heritage

1 Introduction

The analysis of cultural heritage objects relies on multiple techniques of which contactless analysis techniques are favored. Two such optical techniques are multispectral imaging and 3D digitization. Both are increasingly used to document and analyze cultural heritage objects. Multispectral imaging systems are used to produce more faithful color reproductions [2], for pigment identification [10] or to decipher overwritten text in palimpsests [5] for example. On the other hand, 3D models can be used to observe the surface structure of an object without manipulating it. This is useful both for conservators and for communication purposes. Art scholars can examine fine brushstrokes on paintings and chisel marks of statues. 3D models can also be used to create virtual museums and as virtual archives of an object. 3D digitization and multispectral imaging provide complementary data and it is interesting for conservators to be able to visualize both datatypes in an integrated frame. 3D models with multispectral texture can also be used for web-museums or enhanced reality applications.

Systems which simultaneously perform the 3D digitization on an object and acquire multispectral texture [9, 14] generally do not reach the resolution each system can achieve independently. These systems are also very bulky and not transportable. Using

separate systems for the multispectral acquisitions and the 3D digitization of a given object we benefit from the high resolution each acquisition system offers. We can also choose and adapt each acquisition system independently to the present application. This approach, however, requires to register the acquisitions in a single coordinate system. We develop a registration strategy based on close-range photogrammetry techniques to precisely asses the position and orientation of each acquisition system during its use. This paper presents a description of the registration strategy and simulation results for two real scenarios. The strengths of our multimodal registration method are:

- A method suitable for registering data with no salient features
- A registration precision independent from the content of the acquired data
- A registration method which works for many different optical sensors
- A flexible solution suitable for many different applications

2 Related Work

2D-3D registration If the various bands that form a multispectral acquisition have been properly calibrated and registered, registering a multispectral acquisition on a 3D model is equivalent to image to 3D registration. Most 2D-3D registration techniques have the same global setup: first estimate the external camera parameters (position and orientation) of the 2D acquisition system as well as its focal length and possibly other internal parameters (lens distortion, principle point, etc); then use these parameters to project the image on the 3D model.

If we have a set of corresponding points in the two datasets, a calibration method such as Tsai's [15] can be used to estimate the camera parameters. These pairs of 2D-3D points can be natural features, or targets that are added to the scene to guide the registration. There are several drawbacks to this approach: Manually detecting corresponding points is time-consuming, yet the accuracy of the registration depends on this task. Also, image vision algorithms can rarely be used to automatically detect corresponding points due to the very different data structure. When studying cultural heritage objects we have the additional problem that often few natural salient features are present in both the 2D and 3D datasets, yet we can not use targets as they may damage the fragile and unique surfaces.

Another strategy to estimate the camera parameters is based on the maximization of mutual information developed in the late 1990s [8, 16]. Here we compare successive views of the 3D model to the image and iteratively compute the camera parameters. The precision of the ensuing registration is of the order of a few pixels, though the success of such methods greatly depends on the rendering strategy (depth map, silhouette, illumination related, etc.) as illustrated in [4].

Our approach differs in that we evaluate the camera parameters using photogrammetric techniques, instead of interpolating them from the acquired data.

Photogrammetric Tracking Photogrammetric tracking is used in industrial settings for the real-time calibration of robot arms. Two setups exist: either a calibrated camera is fixed to the arm and observes the background which has been covered with targets

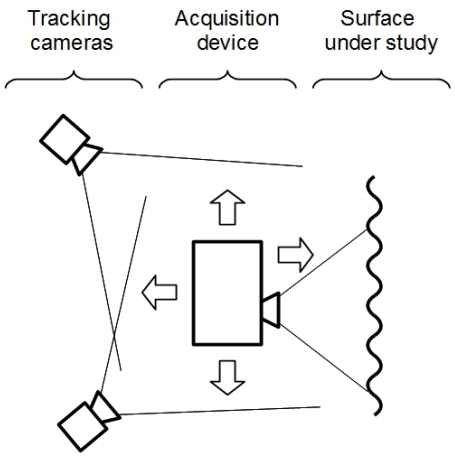

Fig. 1. Setup of the on-site acquisitions: a group of photogrammetric cameras observe each acquisition device while it images the surface from several positions.

[6], or a target object is attached to the robot arm which is observed by several photogrammetric cameras surrounding the scene [7, 13]. Our work is based on the second approach: multiple photogrammetric cameras observe an acquisition system defined by several targets. A similar setup has been used in [3] to guide the 3D registration procedure of a high precision scanner using a second scanner. We extend the scope of this setup to multimodal registration and demonstrate its flexibility and adaptability to several acquisition settings.

3 Material and Methods

3.1 Acquisition Pipeline

Fig. 1 represents the in-situ acquisition setup: a group of photogrammetric/tracking cameras observe the acquisition devices as they successively digitize the surface under study from various positions. Several calibration and acquisition steps are necessary before, during and after the acquisition process to obtain a precise registration.

Pre-processing The following two steps must be performed independently for each acquisition system, either before or after the on-site acquisitions.
- Acquisition system characterization: the relative position of the targets on the acquisition system is measured by taking multiple photos of the acquisition system with several surrounding targets as well as at least one scale bar.
- Acquisition system calibration: a calibration procedure provides us with the interior camera parameters of each acquisition system.

On-site acquisitions The following steps must be performed once the photogrammetric cameras are set up to observe the acquisition devices in all their planned positions.

  - Calibration of the photogrammetric cameras: the standard procedure of taking several simultaneous images of a target plate in many positions provides us with the interior and exterior camera parameters.
  - Data acquisitions: simultaneously from the acquisition system in use and all tracking cameras.

Data-processing We now have the data necessary to perform the registration. This is done in two steps:

  - The photogrammetric cameras interior and exterior orientation, the acquisition system characterization and the view of the acquisition system by the tracking cameras during the acquisition process are used to compute the position and orientation of each acquisition system for each acquisition.
  - The acquisition system calibration and the position and orientation of each acquisition system in the same coordinate system enable us to project all the object data in a common coordinate system.

The precision of the final registration depends on many parameters such as the number, focal length, position and sensor of the photogrammetric cameras; the dimension of acquisition area, etc. Simulations enable us to test many configurations and evaluate how precisely we can detect the position and orientation of each acquisition system.

3.2 Simulation Pipeline

We use a three stage simulation pipeline to predict how precisely we can track the position of each acquisition system. We start by creating a scene under 3ds Max which contains the object under study, an acquisition device in different positions and the photogrammetric cameras. Each acquisition device is simplified by a box modelized by a variable number of points. These points represent the targets that we will attach to our acquisition device. The scene is exported as a *.WRL file and read by a lab-developed software. This software calculates the images seen from each camera as given by the focal length defined in 3ds Max. Lens distortion parameters can be entered manually. This software is also used to add Gaussian noise to the following four scene parameters:

Object coordinates: the coordinates of the targets that define the object in the coordinate system defined by the photogrammetric cameras. These are usually known with a precision of 0.1 mm or 0.05 mm.

Picture coordinates: the coordinates of the targets in the images taken by the photogrammetric cameras. These are usually known with a precision of 1/10 of a pixel. If the conditions are good (sufficient contrast and focus, well resolved targets) the picture coordinates can be resolved with an accuracy of 1/30 of a pixel.

Camera translation: the position of the photogrammetric cameras (X, Y, Z coordinates). The accuracy of these values depends on the camera setup and the results of the calibration procedure. We can usually resolve them with an accuracy better than 0.05 mm.

Camera rotation: the orientation of the photogrammetric cameras (Ω, Φ , K coordinates). We usually know these coordinates with an accuracy better than 0.05 mrad though this also depends on the success of the camera calibration.

The resulting data is then exported as a *.axo file to be treated by a lab-developed software based on the AXOri library [1]. This library can perform the inverse calculation of the camera positions, their interior orientation or the object position, depending on the input parameters.

3.3 Acquisition Systems

Multispectral cameras The multispectral acquisitions are performed either by a lab-designed multispectral camera or with a commercial camera from FluxData (FD-1665-MS). A few characteristics of both cameras are given in the top portion of Table 1. The lab-designed mulitpsectral camera is based on a filter-wheel and has been used in the past to document these objects. Careful calibration and a neural network algorithm provide us with a reflectance spectra for each pixel [12]. On the other hand, the FluxData camera is based on a 3 CCD system which provides simultaneous data for each spectral band. This camera acquires less spectral bands than the lab-designed multispectral camera, but the bigger sensor and pixel size will allow us to register the data more precisely.

3D digitizing system The digitizing of the surface is carried out by a commercial fringe projection system (Atos III, manufactured by GOM). The system can digitize a field of view of $500 \times 500\,\mathrm{mm}^2$ with a resolution of $0.25\,\mathrm{mm}$. A smaller field of view of $150 \times 150\,\mathrm{mm}^2$ can be acquired with a resolution of $0.07\,\mathrm{mm}$.

Photogrammetric cameras The grayscale cameras we use have a 5 megapixel sensor (AVT Stingray F-504B). This 2/3" sensor is large enough to ensure good results, while still being compatible with good quality optics (we use an $8\,\mathrm{mm}$ Pentax lens).

3.4 Objects under Study

This work stems from the need to study both the surface structure and the spectral properties of two cultural heritage objects: a sandstone sarcophagus and a wall painting.

We are interested in monitoring the deterioration of the surface of a polychrome sandstone sarcophagus from the 3$^{\mathrm{rd}}$ century A.D. This sarcophagus is in a crypt under the Friedhofs chapel of the St. Matthias abbey in Trier (Germany). The sarcophagus was discovered by archaeologists approximately fifty years ago. Unfortunately, the airflow and humidity in the crypt has been damaging the surface and fragmentary remains of polychromy. The area of the sarcophagus facing the entrance of the chamber is very damaged. Traces of polychromy on the surface of the sarcophagus are flaking while the stone itself erodes. We study an area of approximately $40 \times 70\,\mathrm{cm}^2$ on this face. Our goal is to precisely localize and quantify the structural and spectral degradation of the sandstone and polychromy in this zone. The need to precisely register the two datasets stems naturally from the will to find correlations in the structural and spectral aging of the surface.

We also monitor a 16$^{\mathrm{th}}$ century wall painting located in the Brömser Hof in Rüdesheim (Germany). In 2008 this wall painting was partially restored. Regular acquisition

campaigns on both the restored and non-restored surfaces are being carried out to compare the aging of these two areas. Once again, the changes that can arise over time are both spectral and structural. This accounts for the complementary acquisition techniques and the need to register the data an integrated dataset.

4 Results and Discussion

The simulation proceeds in three steps: First we optimize the camera arrangement for a given number of cameras observing the acquisition system. This is done while adding noise only to the picture coordinates. Once an optimized setup has been found, we simulate the camera calibration. This tells us how precisely we can expect to evaluate the interior and exterior camera parameters on site. We use the output values to define reasonable noise to add to the camera parameters in the next step. We can then simulate the full tracking procedure with realistic noise. If we do not reach our target goal at this stage, there are other parameters that can be tweaked, such as the number of targets that define the acquisition system. The full strategy is illustrated in detail in the case of the sarcophagus. For the wall painting configuration, we only present a few intermediate results.

4.1 Sarcophagus

Accuracy goal We assume the acquisition system is 50 cm from the acquisition surface of the sarcophagus. The field of view and pixel size at this distance for each multispectral camera are given in the second section of Table 1. We need 3×6 acquisitions to cover the full area of interest with sufficient overlap using the lab-designed multispectral camera (and 4×8 acquisitions using the FluxData multispectral camera). We do not perform the simulations for every 18 (respectively 32) positions. Instead, we calculate the achieved accuracy for the four corners of the rectangle thus defined, as well as for the central position. All results correspond to the worst spatial accuracy in X, Y or Z and the worst angular accuracy achieved in Ω, Φ or K over all the test positions.

Our goal is to register the multispectral data on the 3D model with an accuracy of at least half a pixel. We must thus track the imaging systems with an accuracy better than half a pixel of the multispectral camera in use. This constraint is harder to achieve with the lab-designed multispectral camera which has smaller sensor cells (see the first section of Table 1). It is also generally much harder to reach the desired angular accuracy than the desired spatial accuracy. Our goal is thus to detect the lab-designed multispectral camera with an angular accuracy of 0.128 mrad. Given the size of the area of interest, we would like to reach this target value using no more than four photogrammetric cameras.

Optimizing the camera arrangement In these simulation runs the acquisition device is modelized by a box defined by 26 points. The dimensions of the box are that of the lab-designed multispectral camera. During this simulation phase we only add noise to the picture coordinates, with a standard deviation of 1/10 of a pixel (0.345 µm). The successive setups are described bellow. As can be seen in the corresponding simulation results (Table 2), varying the camera positions does not greatly alter the results.

Table 1. Characteristics of the multispectral images and simulation goal to detect each acquisition systems with half a pixel accuracy. The target value is typeset in boldface.

	Object – sensor distance	Lab-designed multispectral camera	FluxData multispectral camera	
Sensor size		1392×1040	659×494	$\left(\text{pixels}^2\right)$
Cell size		6.45	9.9	(μm)
Focal length		25	25	(mm)
Angular accuracy goal		$\mathbf{0.128}$	0.198	(mrad)
Field of view	$0.5\,\text{m}$	178×134	130×98	$\left(\text{mm}^2\right)$
Pixel size on object	$0.5\,\text{m}$	0.129	0.198	(mm)
Spatial accuracy goal	$0.5\,\text{m}$	0.064	0.099	(mm)
Field of view	$1.8\,\text{m}$	641×482	469×352	$\left(\text{mm}^2\right)$
Pixel size on object	$1.8\,\text{m}$	0.464	0.713	(mm)
Spatial accuracy goal	$1.8\,\text{m}$	0.232	0.356	(mm)

Table 2. Optimizing the camera arrangement to track the lab-designed multispectral camera in front of the sarcophagus. The best results are typeset in boldface.

Camera Arrangement	Results Spatial (mm)	Results Angular (mrad)	Mean number of visible points per camera Camera 1	Camera 2	Camera 3	Camera 4
(a)	0.021_8	0.326	19	19	18.2	16.6
(b)	0.021_2	0.334	19	19	18.2	18.2
(c)	$\mathbf{0.021_0}$	$\mathbf{0.300}$	19	18.8	17.4	17.4
(d)	0.024_0	0.342	19	19	17.4	17.4
(e)	$\mathbf{0.020_0}$	$\mathbf{0.312}$	19	19	17.4	17.4

(a) Initial setup created by placing the cameras roughly at $90°$ angles (top row of Fig. 2). This configuration is based on the authors experience as well as general guidelines in close range photogrammetry such as those given by [11]. We notice that camera 4 is not very well placed, as it only sees a mean of 16.6 points over the five positions. Since the lowest position of the acquisition device is on the ground, it is not possible to place the bottom cameras as low as we would like to. The bottom tracking cameras are constrained to $10\,\text{cm}$ to $20\,\text{cm}$ above the ground and thus detect less points than the top two. On the other hand, raising the top two cameras would reduce the number of points that are well detected by all cameras, an essential factor for a stable configuration.

(b) Based on setup (a), cameras 2 and 3 are placed symmetrically to cameras 1 and 4 with respect to the y-z plane. As could be expected the results are worse, though more points are detected than in the previous setup.

(c) Based on setup (a), cameras 1 and 4 are positioned symmetrically to cameras 2 and 3 with respect to the y-z plane. The results are greatly improved, though camera 2 does not see as many points as it could.

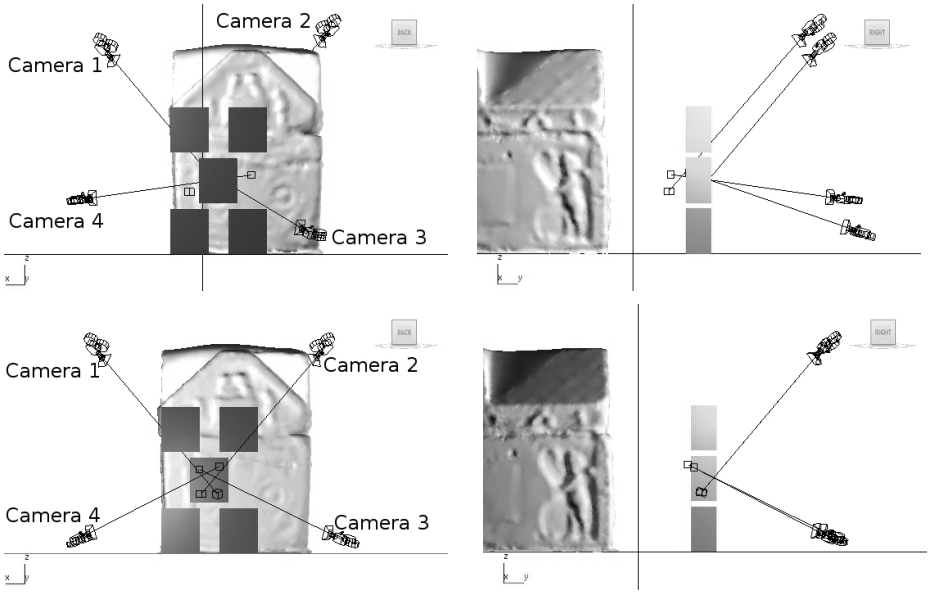

Fig. 2. Top row: view of camera arrangement (a), first configuration. Bottom row: view of camera arrangement (e), optimized configuration.

Table 3. Orientation results for the sarcophagus configuration.

Noise		Results		Characteristics of next input noise		
Picture Coord. (pixel = µm)		Spatial (mm)	Angular (mrad)	Camera Transl. (mm)	Camera Rot. (mrad)	Description
1/10	0.345	0.021_0	0.030	0.03	0.04	Strong constraints
1/30	0.115	0.007_0	0.010	0.01	0.02	Low constraints

(d) Cameras 1 and 2 from setup (b), cameras 3 and 4 from setup (c). Taking what seems like the best from the two previous setups surprisingly gives worse results.
(e) Based on setup (c), we increase the perpendicularity of the intersections (bottom row of Fig. 2). The angular results are not increased but camera 2 detects more points. We thus base the following simulations on this setup.

Orientation To define how precisely we can detect the position and orientation of the cameras during a real calibration we simulate positioning several target fields in the area between the cameras and the sarcophagus. These simulations are also performed by adding noise only to the picture coordinates. We evaluate how accurate the calibration is if the picture coordinates are resolved with a precision of 1/10 of a pixel and 1/30 of a pixel. Adding a reasonable margin to these results defines a realistic amount of noise to use on the subsequent simulations (see Table 3) .

Table 4. Simulation results for the sarcophagus configuration. The results that are better than our target angular accuracy are typeset in boldface.

Object	Noise parameters					Results	
	Picture Coord. (pixel = μm)		Object Coord. (mm)	Camera Transl. (mm)	Camera Rot. (mrad)	Spatial (mm)	Angular (mrad)
Lab MSC						0.020_0	0.312
FluxData MSC	1/30	0.115	0.05	0.01	0.02	0.020_0	0.580
Gom Atos III						0.021_6	0.252
Frame 1	1/30	0.115	0.05	0.01	0.02	0.019_2	0.132
Frame 2						0.014_0	**0.100**
Frame 2	1/30	0.115	0.1	0.01	0.02	0.026_2	0.184
	1/10	0.345	0.1	0.03	0.04	0.032_8	0.230

Table 5. External dimensions of the acquisition systems

Acquisition system	Width (mm)	Height (mm)	Depth (mm)
Lab designed multispectral camera	270	320	180
FluxData multispectral camera	92	112	187
GOM Atos III 3D digitization system	490	170	300

Simulations with realistic noise We apply the lowest realistic noise (strong constraints) to three boxes of the dimension as the acquisition systems (these dimensions are given Table 5) defined by 26 points. The results are given in the top section of Table 4. The target spatial accuracy is reached for all three acquisition systems and its value is hardly influenced by the the dimension of the acquisition system. The target angular accuracy on the other hand is not reached and depends on the size of the acquisition device. Big objects are tracked with a better angular accuracy than small objects. If our acquisition systems were large enough, we could thus detect them with the angular accuracy we seek. We can enlarge the acquisition systems by fixing them to a three-dimensional frame which will also support the targets. We thus evaluate how precisely we can detect a $500 \times 500 \times 500\,\mathrm{mm}^3$ cube covered with 26 targets (Frame 1) or 56 targets (Frame 2). The second section of Table 4 shows that this higher amount of targets is necessary to reach the desired angular accuracy. The third section of Table 4 shows that we need to ensure the best acquisition conditions possible to reach our goal: if we increase the noise added to the parameters, we no longer reach the target angular accuracy.

4.2 Wall Painting

Our goal is once again to register the data with an accuracy better than half a pixel. We are interested in an area that is $2 \times 1.5\,\mathrm{m}^2$. We assume that the multispectral cameras are $1.8\,\mathrm{m}$ from the wall surface. At this distance, we need 16 acquisitions to cover the

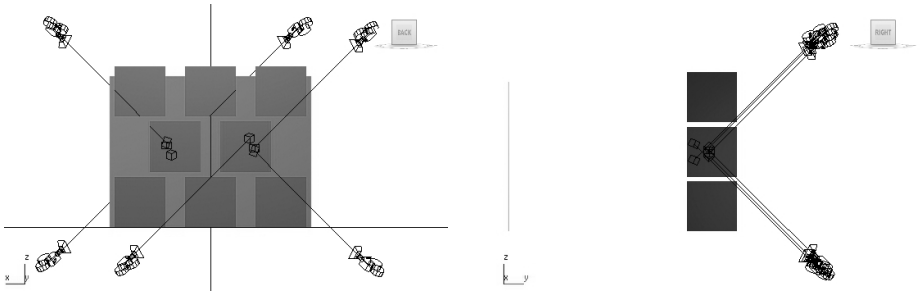

Fig. 3. View of the optimized camera arrangement in front of the wall painting.

full area of interest with the lab-designed multispectral camera and 25 acquisitions to cover the full area of interest with the FluxData multispectral camera.

We start by optimizing the camera arrangement. These simulations are performed using Frame 2. The optimized arrangement with four cameras (see the top section of Table 6) has an angular accuracy which is very far from our target goal, even though we only apply noise to the picture coordinates. We thus use 6 cameras to track the frame in front of the area of interest. Since we know that using more than four cameras to observe the same area does not greatly improve the tracking accuracy, we divide the observed area in two overlapping zones, each of which is observed by 3 cameras. The optimized arrangement is illustrated Fig. 3. The angular accuracy thus achieved is greatly improved.

We now evaluate how precisely the camera calibration can be performed for this setup. The spatial results are a factor two worse than those achieved for the setup in front of the sarcophagus while the angular results are only slightly worse (see the second section of Table 6).

As previously, we use these results to define realistic noise to add to the full setup. Once again, we reach our angular accuracy goal only if we can detect the picture coordinates with an accuracy of 1/30 of a pixel and the object coordinates with an accuracy of 0.05 mm. These are strong but achievable constraints.

The final results are valid if we move the full setup (photogrammetric cameras and acquisition systems) closer to the wall painting. However, as we move closer to the wall painting, the size of a pixel on the object decreases. If the acquisition system is too close to the object the constraining value to reach our accuracy goal of half a pixel will be the spatial accuracy instead of the angular accuracy. In the final setup, the spatial accuracy reached is 0.0152 mm. This value is larger than half a pixel as long as the distance between the wall painting and the lab-designed multispectral camera is more than 12 cm. This distance is even smaller for the FluxData multispectral camera. Using 6 photogrammetric cameras we can thus track our acquisition systems with a precision better than half a pixel in front of any area of $2 \times 1.5\,\mathrm{m}^2$ that is at least 12 cm away from the object.

Table 6. Simulation results for the wall painting configuration.

	Number of cameras	Noise parameters				Results	
		Picture Coord. (pixel = µm)	Object Coord. (mm)	Camera Trans. (mm)	Camera Rot. (mrad)	Spatial (mm)	Angular (mrad)
Camera positioning	4	1/10 0.345	0	0	0	0.013_8	0.208
	6					0.016_4	0.116
Orientation	6	1/10 0.345	0	0	0	0.040_8	0.036
	6	1/30 0.115	0	0	0	0.013_8	0.012
Full results	6	1/10 0.345	0.1	0.05	0.04	0.029_2	0.200
	6	1/30 0.115	0.1	0.02	0.02	0.023_0	0.156
	6	1/30 0.115	0.05	0.02	0.02	0.015_2	**0.106**

5 Conclusion and Future Work

Simulations show that we can to evaluate the position and orientation of an acquisition system in front of an area of $40 \times 70\,\mathrm{cm}^2$ with an angular accuracy of $0.100\,\mathrm{mrad}$ and a spatial accuracy of $0.05\,\mathrm{mm}$ using four cameras photogrammetric cameras. Using six cameras we reach comparable results ($0.106\,\mathrm{mrad}$ angular accuracy and $0.015\,\mathrm{mm}$ spatial accuracy) for an area of $2 \times 1.5\,\mathrm{m}^2$. These configurations will enable us to project multispectral data (or any 2D information) on a 3D model with an accuracy better than half an image pixel.

These simulation results will be validated through a series of lab tests. Then, we will test our technique on the two cultural heritage objects which motivated this study. Though only very specific results are given, this technique is widely adaptable to other setups and different constraints. Furthermore, the technique works independently from the acquisition systems used, as long as they are based on optical sensors that can be characterized and calibrated. This setup could thus be extended to other applications.

Acknowledgments. The authors would like to thank the Conseil Régional de Bourgogne (France) and i3mainz laboratory (Germany) for their financial support. We also thank the Institut für Stein Konservierung (Germany) for providing the test objects and defining the conservation problem.

References

1. Axori photogrammetric bundle block adjustment, `http://www.axios3d.de/produkte/funktionlibs/ori/index_en.html`
2. Berns, R.S.: Color-Accurate Image Archives Using Spectral Imaging. In: Proceedings of the National Academy of Science - Scientific Examination of Art: Modern Techniques in Conservation And Analysis. pp. 105–119 (2005)
3. Blais, F., Taylor, J., Beraldin, J.A., Godin, G., Cournoyer, L., Picard, M., Borgeat, L., Dicaire, L., Rioux, M., Lahanier, C., Aitken, G.: Ultra-High Resolution Imaging at 50 μm

using a Portable XYZ-RGB Color Laser Scanner. In: International Workshop on Recording, Modeling and Visualization of Cultural Heritage (2005)
4. Corsini, M., Dellepiane, M., Ponchio, F., Scopigno, R.: Image-to-Geometry Registration: a Mutual Information Method exploiting Illumination-related Geometric Properties. Computer Graphics Forum 28(7), 1755–1764 (Oct 2009)
5. Easton Jr., R.L., Knox, K.T., Christens-Barry, W.A.: Multispectral imaging of the Archimedes palimpsest. In: Proceedings of the 32nd Applied Imagery Pattern Recognition Workshop. pp. 111–116. IEEE (2003)
6. Hefele, J.: Real-time photogrammetric algorithms for robot calibration. International Archives of Photogrammetry and Remote Sensing XXXIV(Part 5), 33–38 (2002)
7. Maas, H.G.: Dynamic photogrammetric calibration of industrial robots. In: Proceedings of SPIE Vol 3174, Videometrics V. pp. 106–112. SPIE, San Diego, CA, USA (1997)
8. Maes, F., Collignon, A., Vandermeulen, D., Marchal, G., Suetens, P.: Multimodality image registration by maximization of mutual information. IEEE Transactions on Medical Imaging 16(2), 187–98 (Apr 1997)
9. Mansouri, A., Lathuiliere, A., Marzani, F., Voisin, Y., Gouton, P.: Toward a 3D Multispectral Scanner: An Application to Multimedia. IEEE MultiMedia 14(1), 40–47 (2007)
10. Pelagotti, A., Del Mastio, A., De Rosa, A., Piva, A.: Multispectral imaging of paintings. IEEE Signal Processing Magazine 25(4), 27–36 (2008)
11. Remondino, F., El-Hakim, S.: Image-based 3D modelling: a review. The Photogrammetric Record 21(115), 269–291 (Sep 2006)
12. Sanchez, M., Mansouri, A., Marzani, F.S., Gouton, P.: Spectral reflectance estimation from multispectral images using neural networks. In: Physics in Signal and Image Processing. Toulouse, France (2005)
13. Schütze, R., Raab, C., Boochs, F., Wirth, H., Meier, J.: Optopose - a multi-camera system for fast and precise determination of position and orientation for moving effector. In: 9th Conference on Optical 3D Measurement Techniques. Vienna, Austria (2009)
14. Sitnik, R., Mczkowski, G., Krzeslowski, J.: Integrated shape, color, and reflectivity measurement method for 3D digitization of cultural heritage objects. In: Proceedings of SPIE Vol. 7526, 3D Image Processing and Applications. pp. 75260Q 1–10. SPIE, San Jose, CA, USA (2010)
15. Tsai, R.: A versatile camera calibration technique for high-accuracy 3D machine vision metrology using off-the-shelf TV cameras and lenses. IEEE Journal on Robotics and Automation 3(4), 323–344 (Aug 1987)
16. Viola, P.A., Wells, W.M.: Alignment by maximization of mutual information. International Journal of Computer Vision 24, 137–154 (1997)